A Quadruply Hydrogen Bonded Heterocomplex Displaying High-Fidelity Recognition

Taiho Park, Eric M. Todd, Shoji Nakashima, and Steven C. Zimmerman*

*Contribution from the Department of Chemistry, Roger Adams Laboratory,
600 South Mathews Avenue, University of Illinois, Urbana, Illinois 61801*

Received July 8, 2005; E-mail: sczimmer@uiuc.edu

Abstract: An exceptionally strong quadruply hydrogen-bonded complex is formed between 2,7-diamido-1,8-naphthyridine **3** (DAN) and the butylurea of guanosine **6** (UG) in chloroform. The UG unit can be prepared in four steps from guanosine on a 10 g scale in excellent yields without chromatographic purification. The association constant ($K_{assoc} \approx 5 \times 10^7$ M^{-1}) for the UG·DAN complex determined by fluorescence energy transfer from the naphthyridine unit of **3** to coumarin 343 covalently linked UG (**18**) is among the highest reported for a neutral DNA base-pair analogue. The weak self-association of DAN ($K_{dimer} < 10$ M^{-1}) and UG (K_{dimer} ca. 200−300 M^{-1}) means that the UG·DAN complex forms with unparalleled fidelity.

Introduction

For building nanoscale structures with near-angstrom precision, DNA duplex formation has proven quite useful.[1] Several factors make it a well-qualified building material for nanotechnology. First, single-stranded DNA can be made by automated methods. Sequences of varying lengths recognize complementary partners with high selectivity and length tunable affinities, and the resulting duplexes have predictable, well-defined structures. Indeed, a broad range of discrete nanoscale objects have been built entirely of DNA via programmed self-assembly.[2]

Despite the many successes outlined above, DNA-mediated assembly does have its drawbacks. Beyond the considerable expense and difficulty in obtaining multigram quantities of synthetic DNA, for many applications the size and polyanionic nature of the double helix can dominate the properties of the assembled structure. For this reason, small molecule recognition systems based on hydrogen bonding can have significant advantages. Numerous systems have been developed in recent years partly inspired by DNA duplex formation and related forms of biomolecular recognition but also with an eye toward nanoscale supramolecular construction.[3] In this regard, one can specify key properties that an ideal recognition system would possess: (1) ready availability in large quantity, low cost, and with minimal synthetic investment, (2) highly stable complex formation, and (3) high fidelity recognition, i.e., minimal

competition from other substances and recognition systems (vide infra). Despite the many synthetic molecular recognition systems available there are remarkably few that possess all three of these desired characteristics.

Two systems that meet criteria 1 and 2 are the UPy dimer, **1·1**, developed by Meijer, Sijbesma, and their co-workers,[4] and our very similar system[5] known as DeAP (deazapterin) **2** that similarly forms a very stable quadruply hydrogen-bonded dimer.[6] The UPy system has been extensively used in supramolecular polymer chemistry[7] and shown to assemble a variety of other structures.[8] We reported that the heterocyclic unit of DeAP **2** is able to adopt two different tautomeric forms but that each can productively assemble and maintain the same spatial arrangement of the ureido substituent (butyl, Bu). In the context of our studies of **2**, we realized that two noncomplementary

(1) (a) Seeman, N. C. *Chem. Biol.* **2003**, *10*, 1151−1159. (b) Samorì, B.; Zuccheri, G. *Angew. Chem., Int. Ed.* **2005**, *44*, 1166−1181. (c) Rosi, N. L.; Mirkin, C. A. *Chem. Rev.* **2005**, *105*, 1547−1562.

(2) (a) Wengel, J. *Org. Biomolec. Chem.* **2004**, *2*, 277−280. (b) Seeman, N. *Nature* **2003**, *421*, 427−431. (c) Niemeyer, C. M. *Curr. Opin. Chem. Biol.* **2000**, *4*, 609−618. (d) Mirkin, C. *Inorg. Chem.* **2000**, *39*, 2258−2272.

(3) Recent reviews: (a) Krische, M. J.; Lehn, J.-M. *Struct. Bond.* **2000**, *96*, 3−29. (b) Meléndez, R. E.; Carr, A. J.; Linton, B. R.; Hamilton, A. D. *Struct. Bond.* **2000**, *96*, 31−61. (c) Zimmerman, S. C.; Corbin, P. S. *Struct. Bond.* **2000**, *96*, 63−94. (d) Kato, T. *Struct. Bond.* **2000**, *96*, 95−146. (e) Prins, L. J.; Reinhoudt, D. N.; Timmerman, P. *Angew. Chem., Int. Ed.* **2001**, *40*, 2382−2426. (f) Sherrington, D. C.; Taskinen, K. A. *Chem. Soc. Rev.* **2001**, *30*, 83−93. (g) Sijbesma, R. P.; Meijer, E. W. *Chem. Commun.* **2003**, 5−16. (h) Sivakova, S.; Rowan, S. J. *Chem. Soc. Rev.* **2005**, *34*, 9−21. (i) Sessler, J. L.; Jayawickramarajah, J. *Chem. Commun.* **2005**, 1939−1949.

(4) Sijbesma, R. P.; Beijer, F. H.; Brusveld, L.; Folmer, B. J. B.; Hirschberg, J. H. K. K.; Lange, R. F. M.; Lowe, J. K. L.; Meijer, E. W. *Science* **1997**, *278*, 1601−1604.

(5) Corbin, P. S.; Zimmerman, S. C. *J. Am. Chem. Soc.* **1998**, *120*, 9710−9711.

(6) Corbin, P. S.; Lawless, L. J.; Li, Z.; Ma, Y.; Witmer, M. J.; Zimmerman, S. C. *Proc. Nat. Acad. Sci. U.S.A.* **2002**, *99*, 5099−5104.

(7) Selected examples: (a) Lange, R. F. M.; Van Gurp, M.; Meijer, E. W. *J. Polym. Sci., Part A: Polm. Chem.* **1999**, *37*, 3657−3670. (b) Folmer, B. J. B.; Sijbesma, R. P.; Versteegen, R. M.; van der Rijt, J. A. J.; Meijer, E. W. *Adv. Mater.* **2000**, *12*, 874−878. (c) Rieth, L. R.; Eaton, R. F.; Coates, G. W. *Angew. Chem., Int. Ed.* **2001**, *40*, 2153-2156. (d) Yamauchi, K.; Lizotte, J. R.; Long, T. E. *Macromolecules* **2003**, *36*, 1083−1088. (e) Hofmeier, H.; El-ghayoury, A.; Schenning, A. P. H. J.; Schubert, U. S. *Chem. Commun.* **2004**, 318−319. (f) Guan, Z.; Roland, J. T.; Bai, J. Z.; Ma, S. X.; McIntire, T. M.; Nguyen, M. *J. Am. Chem. Soc.* **2004**, *126*, 2058−2065. (g) Takeshita, M.; Hayashi, M.; Kadota, S.; Mohammed, K. H.; Yamato, T. *Chem. Commun.* **2005**, 761−763.

(8) Selected examples: (a) González, J. J.; Prados, P.; de Mendoza, J. *Angew. Chem., Int. Ed.* **1999**, *38*, 525−528. (b) Folmer, B. J. B.; Sijbesma, R. P.; Kooijman, H.; Spek, A. L.; Meijer, E. W. *J. Am. Chem. Soc.* **1999**, *121*, 9001−9007. (c) El-ghayoury, A.; Peeters, E.; Schenning, A. P. H. J.; Meijer, E. W. *Chem. Commun.* **2000**, 1969−1970. (d) Ohsaki, K.; Konishi, K.; Aida, T. *Chem. Commun.* **2002**, 1690−1691. (e) Beckers, E. H. A.; van Hal, P. A.; Schenning, A. P. H. J.; El-ghayoury, A.; Peeters, E.; Rispens, M. T.; Hummelen, J. C.; Meijer, E. W.; Janssen, R. A. J. *J. Mater. Chem.* **2002**, *12*, 2054−2060. (f) Ikegami, M.; Ohshiro, I.; Arai, T. *Chem. Commun.* **2003**, 1566−1567. (g) Shao, X.-B.; Jiang, X.-K.; Zhao, X.; Zhao, C.-X.; Chen, Y.; Li, Z.-T. *J. Org. Chem.* **2004**, *69*, 899−907. (h) Zhao, C.-C.; Tong, Q.-X.; Li, Z.-T.; Wu, L.-Z.; Zhang, L.-P.; Tung, C.-H. *Tetrahedron Lett.* **2004**, *45*, 6807−6811.
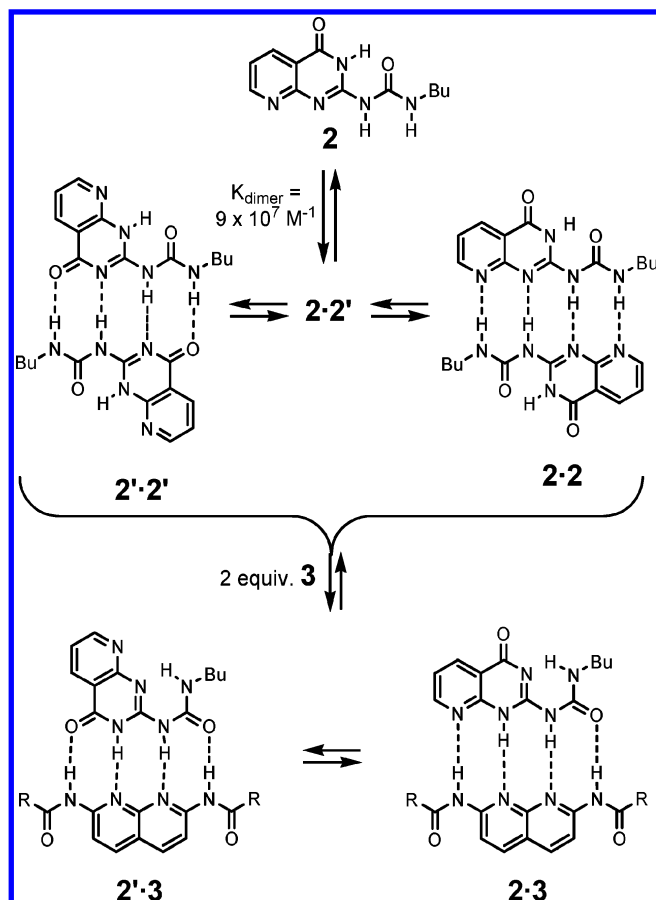
Figure 1. Formation of three strong dimers from DeAP **2** and their quantitative conversion to heterocomplex **2·3** or **2′·3** upon addition of two equivalents of DAN **3**.

forms of **2** also exist which present the ADDA hydrogen bonding array (A = acceptor, D = donor).

By the addition of 2 equiv of 2,7-diamido-1,8-naphthyridine (DAN) **3** to chloroform solutions of DeAP **2**, it was found that heterocomplex **2·3** or **2′·3** was formed exclusively (Figure 1). The ADDA hydrogen bonding array is also available to UPy **1**, and we found a similar heterocomplex with DAN (**1·3**) was formed.[9] The UPy·DAN complex has been independently and extensively studied by Li and co-workers,[10] and very recently it was used to form supramolecular polymers.[11]

From the perspective of their stability and the ready availability of the component modules, the **1·3** and **2·3** heterocomplexes are attractive candidates for use in nanotechnology. However, the ability of **1** and **2** to dimerize lowers the fidelity of the **1·3** and **2·3** system and for many applications this can lead to undesired assembly processes. For this reason we sought an alternative that would display the ADDA hydrogen-bonding array without competition from the AADD array, which strongly dimerizes. Herein we describe the synthesis of guanosine urea **4** (UG) and detailed complexation studies with DAN **3**. The results suggest the **3·4** heterocomplex meets all three criteria

(9) Corbin, P. S., unpublished results.
(10) (a) Zhao, X.; Wang, X.-Z.; Jiang, X.-K.; Chen, Y.-Q.; Li, Z.-T.; Chen, G.-J. *J. Am. Chem. Soc.* **2003**, *125*, 15128−15139. (b) Wang, X.-Z.; Li, X.-Q.; Shao, X.-B.; Zhao, X.; Deng, P.; Jiang, X.-K.; Li, Z.-T.; Chen, Y.-Q. *Chem.−Eur. J.* **2003**, *9*, 2904−2913. (c) Li, X.-Q.; Jiang, X.-K.; Wang, X.-Z.; Li, Z.-T. *Tetrahedron* **2004**, *60*, 2063−2069. (d) Li, X.-Q.; Feng, D.-J.; Jiang, X.-K.; Li, Z.-T. *Tetrahedron* **2004**, *60*, 8275−8284.
(11) Ligthart, G. B. W. L.; Ohkawa, H.; Sijbesma, R. P.; Meijer, E. W. *J. Am. Chem. Soc.* **2005**, *127*, 810−811.

outlined above and is an excellent prospect for use in nanoscale construction.

Results and Discussion

Higher Fidelity Recognition via Tautomeric Fixation. In examation of the **1·3** and **2·3** complexes, it was clear that the methyl and fused pyridine rings played a spectator role (Figure 2a). Thus, alternative substituents or ring fusions might favor the ADDA array at the expense of the AADD form. Given the well-documented tendency for DNA bases to have fixed tautomeric forms attention was focused on ureas of guanosine (i.e., UG **4**). For compounds **1**, **2**, and **4**, five limiting tautomeric and conformation isomers were considered computationally (Figure 2b). In each case, the urea conformation was set as cis, cis, the productive form, and the structure minimized first using molecular mechanics (MMFF) and then the MP2−6-31+G* method with full geometry optimization.[12] The final energies and dipole moments are tabulated in the Supporting Information.
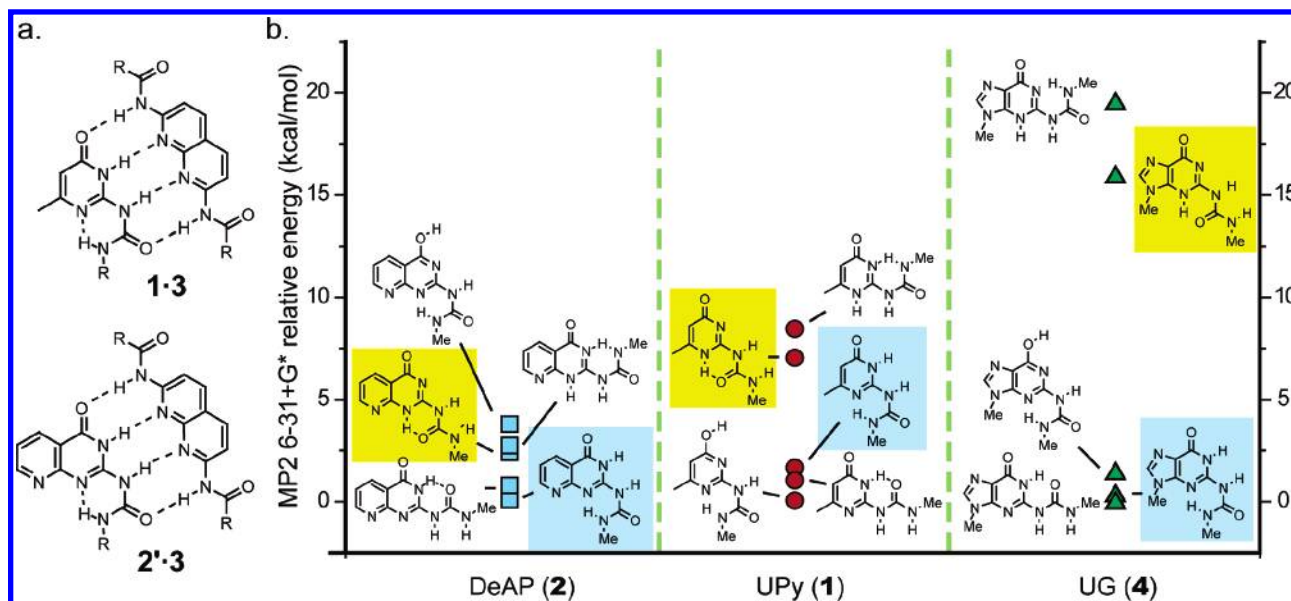
As seen in Figure 2b, the energies of the five different forms of DeAP **2** are tightly clustered, whereas those of UPy **1** are somewhat more spread out. The three lowest energy forms of UG **4** are within 1.4 kcal mol^{-1} of one another, whereas the two remaining are significantly higher in energy. Most importantly, along the series **2 → 1 → 4** the energy of the N1H tautomer, which expresses the strongly dimerizing AADD array (highlighted in yellow in Figure 2b), increases markedly in energy. Of course the calculations performed are in the gas phase so the different forms will be stabilized to different extents in solution. Likewise different computational methods may lead to different relative energies and possibly even different orderings. Nonetheless, despite these uncertainties the striking increase in the calculated energy for the DDAA form of UG, **4d**, relative to the lowest energy form (**4a**) strongly hinted at the desired tautomeric fixation (Scheme 2). The further finding that **4b**, the desired ADDA form, is just 0.3 kcal mol^{-1} higher in energy than **4a** was encouraging although this was tempered by the apparent accessibility of ADAD form **4c**. The analogous tautomer in **1** was shown to be capable of strong dimerization.[13] Overall, the results provided considerable impetus to undertake the synthesis and study of UG **4**.

Synthesis and Structure of UG 4. The initial target was UG **4** (R = 2′,3′-*O*-isopropylidene ribose, R′ = Bu), containing a single unprotected hydroxyl group available for further functionalization. UG **4** could be readily prepared from guanosine in four steps (ca. 76−95% overall yields) on >10 g scale without resorting to chromatography (Scheme 3). The synthesis began with the triacetylation of guanosine using acetic anhydride (Ac$_2$O) in the presence of triethylamine (TEA) and *N,N*-(dimethylamino)pyridine (DMAP).[14] By carrying out the addition of the Ac$_2$O at 0 °C, *N*-acetylation could be suppressed and **5** obtained in a near quantitative yield. Although 2′,3′,5′-triacetylguanosine is commercially available, it is expensive, whereas guanosine is available in bulk for less than a dollar a gram.

Introduction of butyl urea by reaction of **5** with butyl isocyanate is the key step in the preparation of **4**, and it proved

(12) See Supporting Information for details.
(13) Beijer, F. H.; Sijbesma, R. P.; Kooijman, H.; Spek, A. L.; Meijer, E. W. *J. Am. Chem. Soc.* **1998**, *120*, 6761−6769.
(14) Nair, V.; Turner, G. A.; Chamberlain, S. D. *J. Am. Chem. Soc.* **1987**, *109*, 7223−7224.
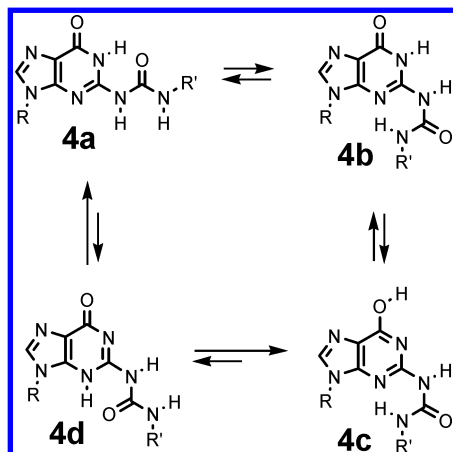
Figure 2. (a) Structure of **1·3** and **2′·3** heterocomplexes showing nonessential role played by methyl substituents (**1**) and fused pyridine ring (**2′**). (b) Calculated relative energies of five different protomers/conformers of **1**, **2**, and **4**. The DDAA form (yellow) is undesired; the ADDA form (blue) is the desired form for heterocomplexation.

Scheme 1
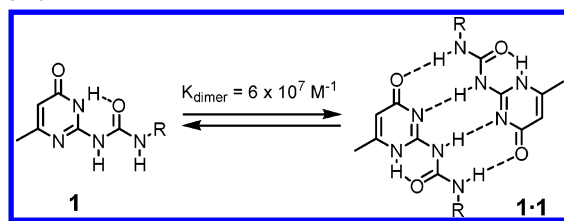
Scheme 2

to be problematic. Heterocyclic amines exhibit lowered reactivity toward isocyanates, but at elevated temperatures they can generally be converted to the desired urea.[5,6,15] Under conditions that were successful previously, **5** did not react with butyl isocyanate. The low reactivity was solved by employing sodium hydride (NaH) to deprotonate the guanosine in DMF. This method allowed the reaction with butyl isocyanate to proceed smoothly giving **6** in 97% yield. The exact site of deprotonation is not known nor is the mechanism by which the NaH activates the reaction. It was important to use slightly less than 1.0 equiv

Scheme 3
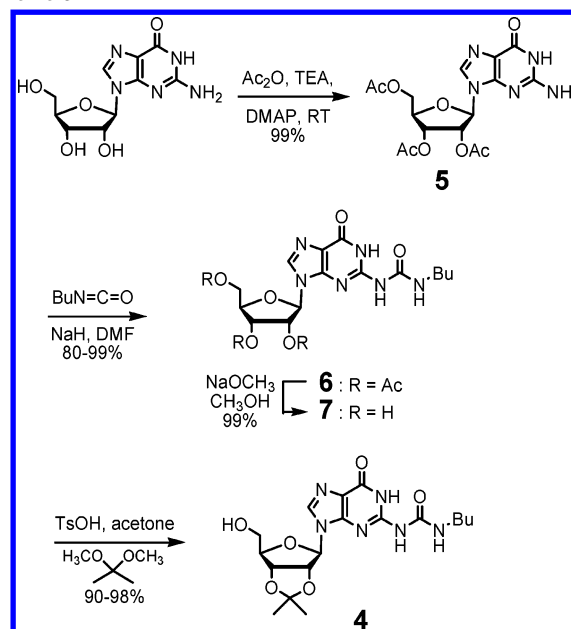
of both NaH and butyl isocyanate to suppress formation of unknown byproducts that otherwise required column chromatography to be removed. Ten separate **5 → 6** conversions were carried out with eight affording product in yields that ranged from 80% to nearly quantitative. Two reactions gave poor to low yield, indicating a degree of irreproducibility, the origin of which has not been identified. Quantitative deacetylation of **6** using sodium methoxide (NaOCH$_3$) afforded **7**, which was protected[16] by 2,2-dimethoxy propane in the presence of *p*-toluenesulfonic acid to give **4** (R = 2′,3′-*O*-isopropylidene ribose, R′ = Bu).

The ribose ring in **4** is not essential to its function but was included both to enhance the solubility of **4** and its synthetic

(15) (a) Corbin, P. S.; Zimmerman, S. C.; Thiessen, P. A.; Hawryluk, N. A.; Murray, T. J. *J. Am. Chem. Soc.* **2001**, *123*, 10475−10488. (b) Corbin, P. S.; Zimmerman, S. C. *J. Am. Chem. Soc.* **2000**, *122*, 3779−3780.

(16) Defrancq, E.; Leterme, A.; Pelloux, N.; Lhomme, M.-F.; Lhomme, J. *Tetrahedron* **1991**, *47*, 5725−5736.
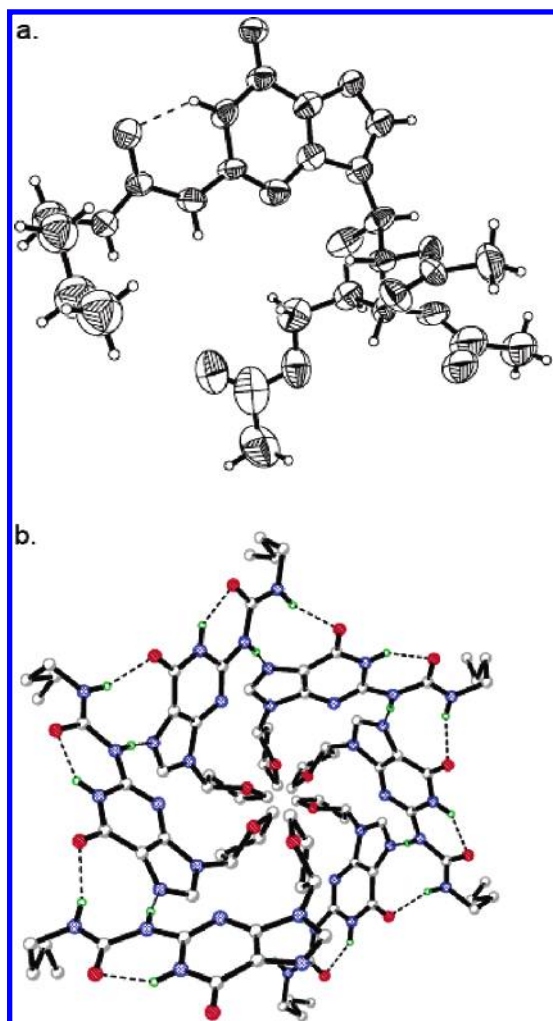
Figure 3. (a) ORTEP diagram from X-ray analysis of **6**. Ellipsoids represent 35% probability. (b) Packing showing infinite helical hydrogen-bonded spiral.

precursors and to provide multiple points for attaching additional functionality. It is very likely that guanine itself and simple structural analogues will function similarly and these are under active investigation.

To gain insight into the structure of **4**, a crystal of **6** suitable for X-ray analysis was grown by slow evaporation of a chloroform solution. The crystal contained disordered solvent molecules as well as a disordered butyl group, but the crystal structure could nonetheless be solved. As seen in Figure 3a, the UG unit adopts a conformation and tautomeric form analogous to **4a** (Scheme 2) which was calculated to be the lowest energy. A table of bond lengths and angles in addition to the cif file is included in the Supporting Information. Beyond confirming the structure, the most important aspect of the X-ray analysis comes from examination of the packing. In particular, both NH groups of the urea moiety hydrogen bond to the Hoogsteen site of a neighboring guanosine nucleus. This leads to a beautiful helical hydrogen-bonded, supramolecular polymer in the solid state (see Figure 3b). The relevance of this interaction to the aggregation state of **4** in solution is discussed below.

Self-Association of UG 6. The UG module was designed to disfavor the **4d** form, which in turn would disfavor the type of highly stable dimers formed by **1** and **2**. The self-association

of **6** was studied in chloroform both by vapor pressure osmometry and ^{1}H NMR. Thus, the ^{1}H NMR of **6** was examined as a function of dilution from 30 to 0.078 mM. Two representative spectra at 0.23 and 30 mM are shown in Figure 4. At 0.23 mM proton resonances corresponding to the NH groups are observed at ca. $\delta = 12.00$, 8.0, and 5.40 ppm. The latter peak is assigned to the aliphatic urea NH group whose position is consistent with non-hydrogen-bonded urea H_1 (▲). The NH resonance at $\delta = 12$ ppm is assigned to an intramolecularly hydrogen bonded H_3 group (■) and the final NH resonance at $\delta = 8.0$ to the heterocyclic urea proton H_2 (●). As the concentration is raised all three *NH* protons move downfield, but H_1 and H_2 were much more so than H_3 (Figure 4c). The former shifts are consistent with the formation of intermolecular hydrogen bonds. The smaller downfield shift seen for H_3 may result from a strengthening of the intramolecular hydrogen bond, which would be expected as the interactions with the Hoogsteen site will further polarize the urea carbonyl group. The dilution curves of H_1 and H_2 were fit to a dimer model giving an average $K_{dimer} = 185 \text{ M}^{-1}$.
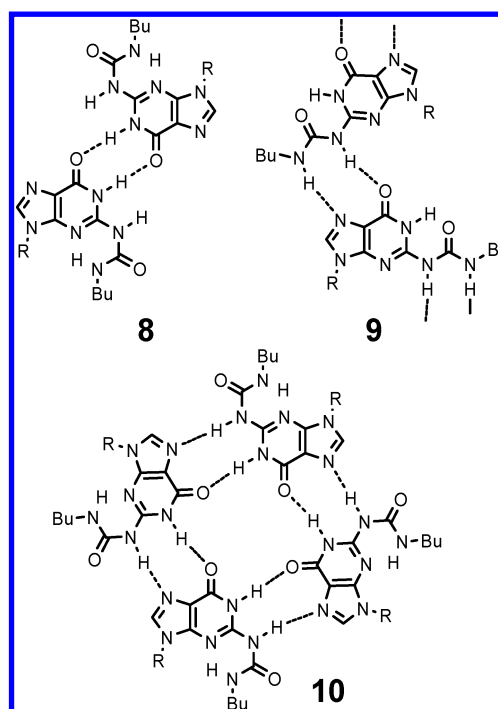

Three ways in which **6** might self-associate are represented by **8**–**10**. Several simple dimers with two intermolecular hydrogen bonds, analogous to **8**, can be envisioned.[17] Oligomeric assemblies[18] such as **9** and cyclic aggregates analogous to the well-studied guanosine tetrad[19] can also be considered. Although a dimerization model fits the data in Figure 4c, the VPO data described below are more consistent with an oligomeric, hydrogen-bonded supramolecular polymer such as **9** or the self-assembled helix seen in the solid state (Figure 3b).

(17) Gallant, M.; Viet, M. T. P.; Wuest, J. D. *J. Am. Chem. Soc.* **1991**, *113*, 721−723.
(18) (a) Guanosine tapes: Giorgi, T.; Grepioni, F.; Manet, I.; Mariani, P.; Masiero, S.; Mezzina, E.; Pieraccini, S.; Saturni, L.; Spada, G. P.; Gottarelli, G. *Chem.−Eur. J.* **2002**, *8*, 2143−2152. (b) General review of hydrogen bonded tapes: MacDonald, J. C.; Whitesides, G. M. *Chem. Rev.* **1994**, *94*, 2383−2420.
(19) (a) Spada, G. P.; Gottarelli, G. *Synlett* **2004**, *4*, 596−602. (b) Davis, J. T. *Angew. Chem., Int. Ed.* **2004**, *43*, 668−698.
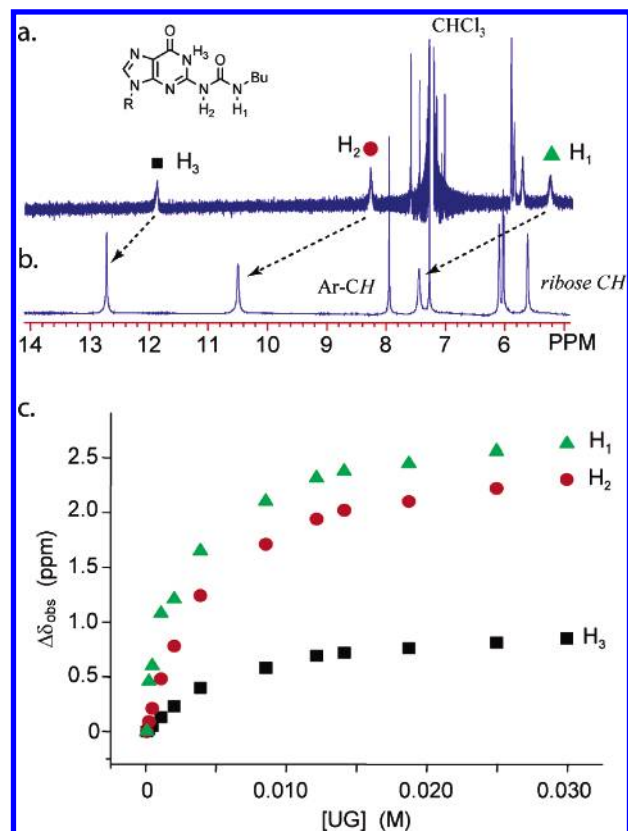
Figure 4. Self-association of **6**: (a and b) ^{1}H NMR at 0.23 mM and 30 mM, respectively (chloroform-*d*, RT). The CHCl$_3$ peak is cut off for clarity in part a. (c) Dilution shifts for NH protons.

Vapor pressure osmometry (VPO) studies of **6** at 30.0 °C in chloroform over the concentration range 15−818 mM were performed to establish the aggregation state in solution and to compare the association strength with that obtained by ^{1}H NMR spectroscopy. The R/C vs C plots are curved but using benzil as a standard and fitting the highest concentration points to a line indicates a MW of about 2000, close to that of a tetramer (MW$_{UG}$ = 508.4). Different possible models for the aggregation of UG were examined more systematically using the method of Schrier.[20] Thus, the VPO data was fit to five limiting models: (a) models 1−4, simple equilibrium between monomer and dimer, trimer, tetramer, or pentamer; (b) model 5, oligomerization with identical stepwise K_a values. In this method, model K_{eq} are calculated at different concentrations with self-consistent values indicating the appropriateness of the model. As seen in Figure 5, the data at multiple concentrations gave poor consistency for models 1−4 but fit well to model 5. An average association constant, K_{eq} = 230 M^{-1}, was obtained consistent with **6** weakly self-associating.

The overall data suggests that UG weakly self-associates by forming hydrogen-bonded multimers. Whatever its precise mode of aggregation, the key finding is that, in contrast to **1** and **2**, UG does not form a stable DDAA-mediated dimer.

Formation and Stability of the UG·DAN Complex. Formation of the UG·DAN complex was readily observed by ^{1}H NMR in chloroform-*d*. As seen in Figure 6, the NH resonances of a 1:1 mixture of **3** (R = C$_6$H$_{13}$) and **6** appeared as four reasonably sharp peaks significantly downfield from their position in the

individual components, DAN and UG. When DAN **3** is in excess its NH resonances appear intermediate between that for free (δ = 8.26 ppm) and complexed (δ = 11.7 ppm) DAN indicating exchange that is fast on the NMR time scale. Likewise, within the **3·6** complex the two DAN NH groups appear as one peak, consistent with either fast exchange or identical environments. It is interesting that at the stoichiometry [DAN]/[UG] = 3 two broad, overlapping NH signals are seen for DAN.

When UG is in excess the situation is considerably more complex. At 10 mM, UG the NH peaks become significantly broader and new NH resonances appear intermediate between free and complexed UG (Figure 6). The data are consistent with free and complexed UG in slow exchange on the NMR time scale, but the exchange rate approaches the NMR time scale. At higher dilution (ca. 0.5 mM) DAN remains in fast exchange with the 1:1 complex, but UG is clearly in slow exchange. Overall, the results are consistent with free UG adopting the **4a** form and undergoing a slow conformational change to the **4b** prior to complexing DAN. In contrast DAN is always in the correct form.

The strength of the DAN·UG complex was apparent from a simple ^{1}H NMR dilution experiment. Thus, when a 1:1 mixture of **3·6** in chloroform-*d* was diluted to 10 μM, no new peaks appeared nor did any shift occur. The spectrum at this concentration exhibits a poor signal-to-noise ratio,[12] but if it is assumed that 20% dissociation would be observed, then a lower limit on the association constant can be placed: K_{assoc} > 2 × 10^6 M^{-1}. Thus, the ^{1}H NMR dilution experiment suggests a highly stable complex.

To study the complexation at lower concentrations, spectrophotometric methods were employed. The UG unit **6** shows no significant absorption above 310 nm, whereas the DAN unit **3** (R = C$_6$H$_{13}$) gives a cluster of peaks in the region λ = 310−350 nm (Figure 7). Upon addition of UG (**6**) to DAN (**3**), a new absorption with λ_{max} = 358 nm is observed which is indicative of complexation. A 1:1 mixture of **3** and **6** in chloroform was diluted to 10 nM using 10-cm UV−vis cells to provide appropriate signals. At the lowest concentrations there was a clear loss of the discrete absorption bands, but the overall appearance of the spectrum did not change, and most importantly the ratio of intensity at λ_{max} = 347 nm to that at λ_{max} = 358 did not increase. As with the NMR studies the results suggested a very strong complex and that a more sensitive technique would be needed to measure the association constant.

Fluorescence resonance energy transfer (FRET)[21] has become an indispensable method to study biomolecular recognition mechanisms.[22] Rebek and co-workers recently reported the use of FRET to characterize both the kinetics and thermodynamics of a strong calixarene dimer (capsule) formation.[23] The donor and acceptor chromophores employed, coumarin 2 and coumarin 343, were the same ones used by Fréchet in the development of light-harvesting dendrimers.[24] On the basis of these prece-

(20) Schrier, E. E. *J. Chem. Edu.* **1968**, *45*, 176−180.

(21) Stryer, L.; Haugland, R. P. *Proc. Natl. Acad. Sci. U.S.A.* **1967**, *58*, 719−726.
(22) Selected recent reviews: (a) Miller, J. N. *Analyst* **2005**, *130*, 265−270. (b) Selvin, P. R. *Nat. Struct. Biol.* **2000**, *7*, 730−734.
(23) Castellano, R. K.; Craig, S. L.; Nuckolls, C.; Rebek, J., Jr. *J. Am. Chem. Soc.* **2000**, *122*, 7876−7882.
(24) (a) Gilat, S. L.; Adronov, A.; Fréchet, J. M. J. *Angew. Chem., Int. Ed. Engl.* **1999**, *38*, 1422−1427. (b) Gilat, S. L.; Adronov, A.; Fréchet, J. M. J. *J. Org. Chem.* **1999**, *64*, 7474−7484. (c) Adronov, A.; Gilat, S. L.; Fréchet, J. M. J.; Ohta, K.; Neuwahl, F. V. R.; Fleming, G. R. *J. Am. Chem. Soc.* **2000**, *122*, 1175−1185. (d) Lee, L. F.; Adronov, A.; Schaller, R. D.; Fréchet, J. M. J.; Saykally, R. J. *J. Am. Chem. Soc.* **2003**, *125*, 536−540.
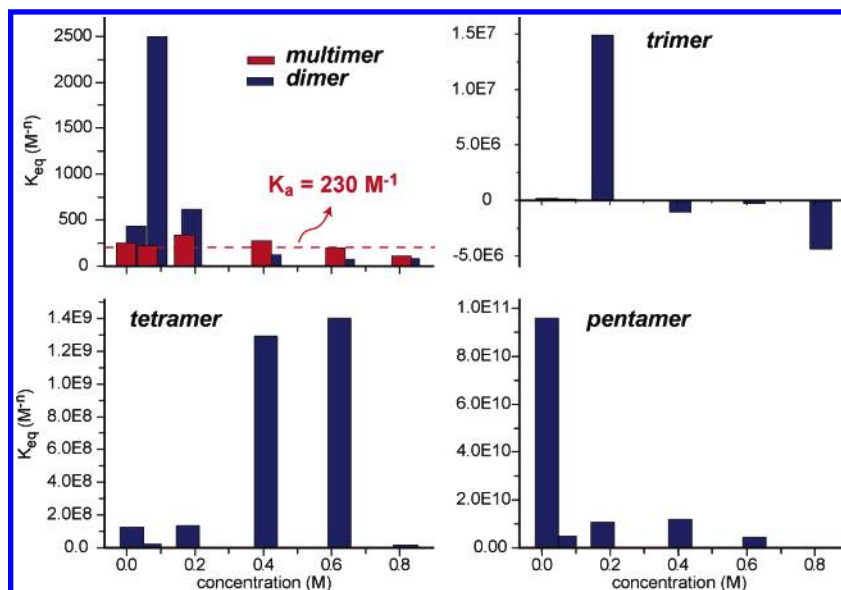
Figure 5. Plots of calculated equilibrium constants at different concentrations from VPO according to different aggregation models.
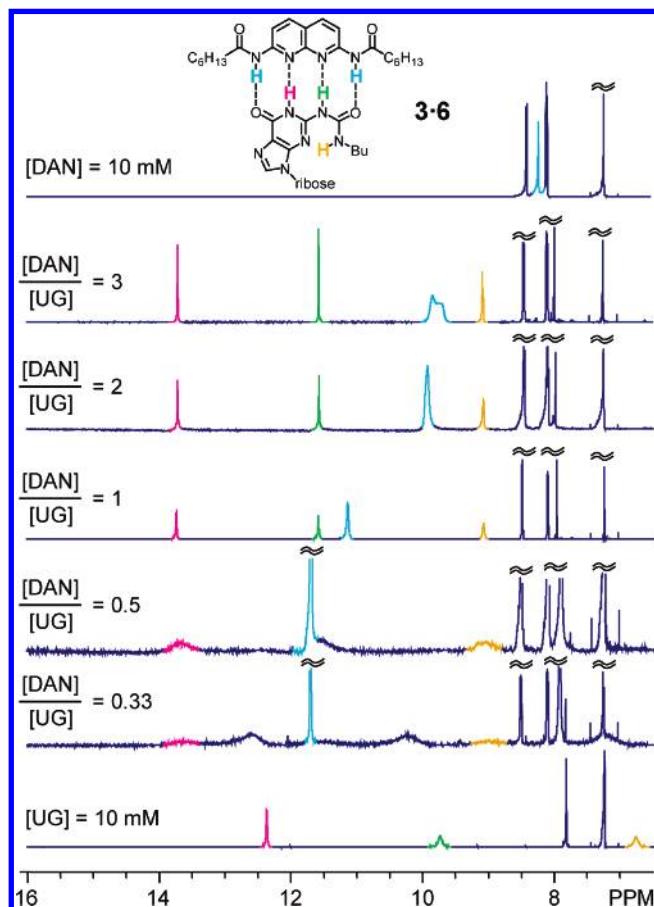

Figure 6. NMR in chloroform-*d* at various DAN/UG ratios (room temp). Minor component fixed at 10 mM. The ca. 0.3 ppm shift of DAN NH observed from [DAN]/[UG] = 1−0.5 may reflect small weighing errors or kinetically slow equilibrium; other 1:1 mixtures showed DAN NH group overlapping UG NH.

dents, target compounds **11** and **12** were synthesized as outlined in Schemes 4 and 5.

The expectation in synthesizing **11** and **12** was that excitation of the coumarin 2 moiety in **11** at $\lambda_{max} = 340$ nm would lead to an emission at $\lambda_{em} = 420$ nm with FRET-mediated excitation of the coumarin 343 group in bound **12** giving complex specific
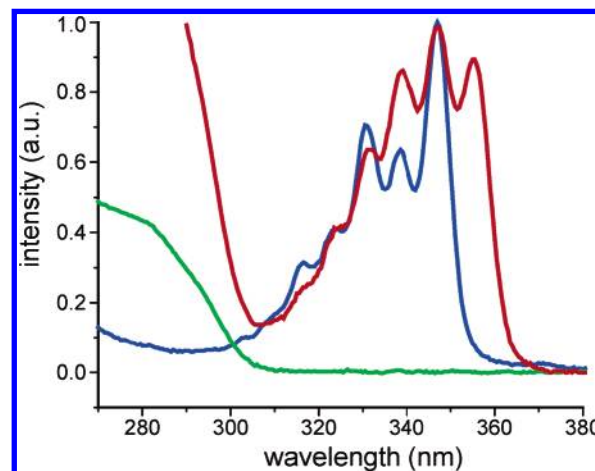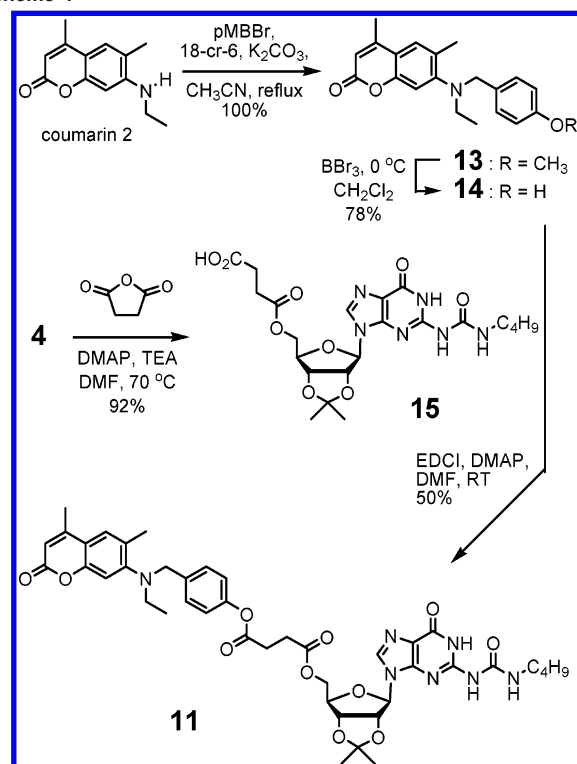
Figure 7. Overlaid UV−visible spectra of 10 μM solution of **3** (blue line), **6** (green line), and a 1:5 mixture of **3·6** (10 μM) in reagent-grade chloroform at room temperature.

emission at $\lambda_{em} = 465$ nm. In the event, excitation at $\lambda_{ex} = 340$ nm was unselective affecting both the coumarin 2 and naphthyridine (DAN) units. The latter appeared to undergo energy transfer to both coumarin units significantly complicating the picture. In examining the UV−visible and fluorescence spectrum of DAN **3** (R = C_6H_{13}) and coumarin 343 they appeared well suited to serve the role of FRET donor (**3**) and acceptor (coumarin 343) (Figure 8a). Thus, compound **18** was prepared in 50% yield by esterifying coumarin 343 with **4**, activating the carboxylic acid group with EDCI and DPTS.
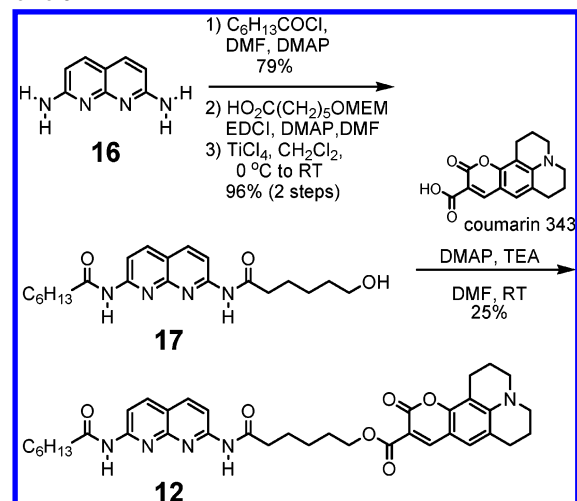
In examination of the fluorescence of 1:1 mixtures of **3** and **18** in chloroform, a significant FRET effect was observed at nanomolar concentrations. Thus, excitation of the naphthyridine unit of **3** at 340 nm led to fluorescence emission at 470 nm corresponding to the coumarin unit of **18**. Under the same conditions minimal emission, typically 10−20% of that seen with **3·18**, was observed when a 1:1 mixture of **3** and coumarin 343 was used. This background fluorescence was believed to originate from direct excitation of coumarin 343 and was subtracted from that observed in the studies of **3·8** (Figure 8c). The control study lacking the UG unit also serves to demonstrate that the FRET results from hydrogen-bond complexation
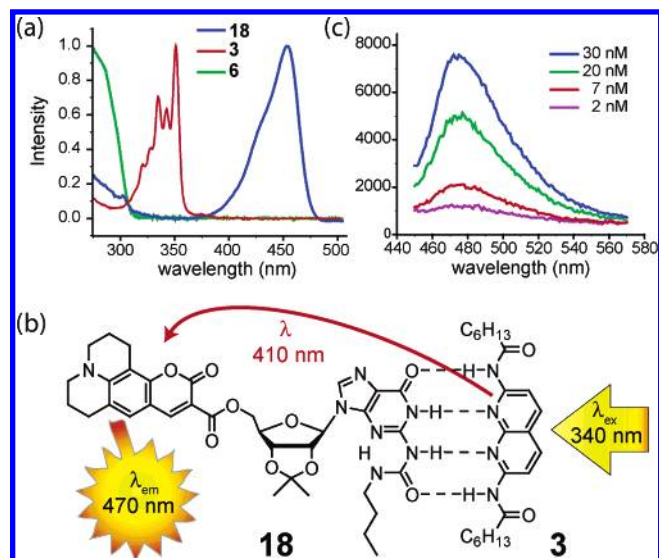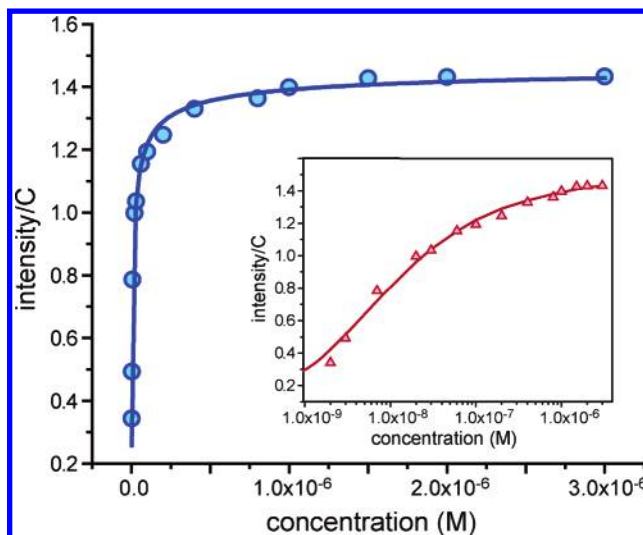
Scheme 4

Scheme 5

Figure 8. (a) UV−visible spectra of **3**, **6**, and **18** in chloroform. (b) Fluorescence emission spectra of **3·18** complex with dilution in chloroform (background subtracted, see text). (c) Schematic showing FRET mechanism in **3·18** complex.


Figure 9. Fluorescence intensity (arbitrary units) plotted against concentration. Inset shows same data on semilog plot. See text and Supporting Information for details about fitting.

mediated by this key recognition unit. The fluorescence dilution data (Figure 9) were fit to eq 1.[12] From three runs, the association constant is estimated to be $K_{assoc} \approx 5 \times 10^7$ M^{-1}, but given the difficulty in obtaining reproducible data at such high dilution, it could be an order of magnitude higher or lower.

$$A = \left([UG]_\circ + \frac{1}{2K_{assoc}} - \sqrt{\frac{[UG]_\circ}{K_{assoc}} + \frac{1}{4K_{assoc}^2}} \right)/[UG]_\circ \quad (1)$$

Fidelity of UG·DAN Complex in Comparison to DeAP· DAN. As noted in the Introduction, both **1** and **2** form highly stable complexes with DAN, but it was noted that the ability of **1** and **2** to form tight dimers can be a disadvantage under certain conditions. We recently examined this issue on a quantitative basis by modeling the *fidelity* of various systems

with multiple complexation equilibria.[25] Fidelity was defined as the ratio of concentration of the desired complexes to the concentration of all associated species. Thus, the fidelity (F) of a system will range from $0 \leq F \leq 1$, where $F = 1$ indicates exclusive formation of desired species and $F = 0$ exclusive formation of undesired associated species. In the case of the UG·DAN complex, the fidelity would be given by eq 2 where the UG self-association ($K_a \approx 200$ M^{-1}) is a more serious threat to the fidelity of the system than the weak DAN dimer ($K_{dimer} < 10$).

$$\text{fidelity } (F) = \frac{[UG \cdot DAN]}{[(DAN)_2] + [(UG)_n] + [UG \cdot DAN]} \quad (2)$$

By use of the reported procedures[25] and treating the UG self-association as a dimerization process, the fidelity of both the

(25) Todd, E. M.; Quinn, J. R.; Park, T.; Zimmerman, S. C. *Isr. J. Chem.* **2005**, *45*, 381−389.
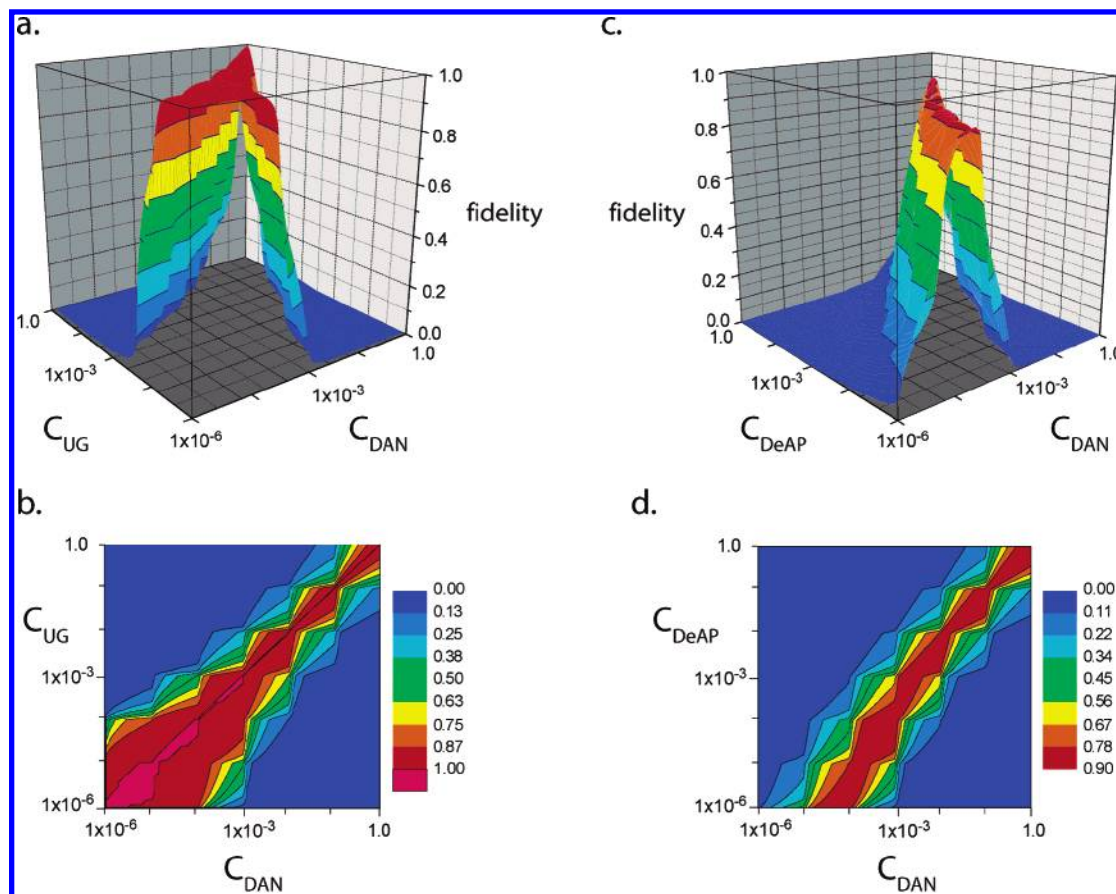
Figure 10. Fidelity plots comparing UG·DAN and DeAP·DAN complexes. C is analytical concentration (M). The latter system and the methods used were published previously.[25]

UG·DAN and DeAP·DAN complexes were modeled over a broad range of concentrations ($1-10^{-6}$ M, Figure 10). Both systems show a ridge of high fidelity that rapidly drops off at highly nonstoichiometric ratios. In the DeAP·DAN system, the ridge is significantly narrower and with dilution curves toward the DAN side. As a result of this curvature the fidelity of a 1:1 mixture of DeAP and DAN, which is only ca. 89% ($F = 0.89$) at 1 M, degrades significantly with concentration so that at 1 mM it has dropped to ca. 63% ($F = 0.63$). In contrast, the UG·DAN complex (1:1 stoichiometry) exhibits a nearly perfect fidelity of >99.9% at 1 M and maintains that level across a 10^6-fold dilution. The high fidelity ridge seen in parts a and b of Figure 10 is significantly wider and does not curve as it does in the DeAP–DAN system. The practical advantage of this property is obvious. The highly stable UG·DAN complex can be expected to form reliably across a broad range of concentrations including those that deviate significantly from 1:1 stoichiometry.

One feature of DNA that makes it particularly useful in creating nanostructures is the ability to synthesize pairs of complementary strands that assemble with high fidelity. This fidelity is inherent in the base pairing, and we previously modeled the simultaneous formation of the G·C base-pair and the T·DAP heterocomplex, an anaolog of A·T that has been used extensively in host–guest and self-assembly studies (Figure 11). The observed fidelity plot exhibits a broad trough of lowered fidelity at 1:1 stoichiometry which dips considerably with dilution. However, these features are seen only because the vertical axis is significantly expanded. Indeed, this system

exhibits very high fidelity ($F > 0.96$) at all concentrations and stoichiometries examined from 1 to 10^{-6} M.

Despite the excellent fidelity shown by the G·C and T·DAP complexes, their free energies of association, ca. 3 and 6 kcal mol^{-1}, respectively, are below that considered optimum for many applications. Thus, it was of particular interest to model the fidelity shown by mixtures of the very strong UG·DAN heterocomplex and the DeAP dimer. To model this pair it was necessary to know the UG·DeAP association constant, which was estimated by ^{1}H NMR titration. Up to 2 equivalents of UG were added to a 1.5 mM solution of DeAP in chloroform-*d*, the K_{assoc} estimated from the ratio of the new complex peaks to those of the DeAP dimer (slow exchange on NMR time scale) and by determining the amount of UG necessary to effect nearly complete loss of the DeAP dimer. The association constant thus obtained, $K_{assoc} = 10^6$ M^{-1}, was considered a conservative estimate useful for modeling, although the actual value could be as much as 10-fold lower.

The fidelity of the UG·DAN/(DeAP)$_2$ system was modeled and is shown in Figure 11b. There is a shallow trough running along the line defining a 1:1 stoichiometry of the hetero and homo complexes, but its minimum still represents a fidelity of $F \geq 0.99$. As were reported previously,[25] the two plateaus at highly nonstoichiometric ratios of the two species is an artifact of the definition of fidelity. Nonetheless, the UG·DAN complex and DeAP dimer appear to exhibit outstanding fidelity and stability, properties which should make them especially useful members of the supramolecular toolkit.
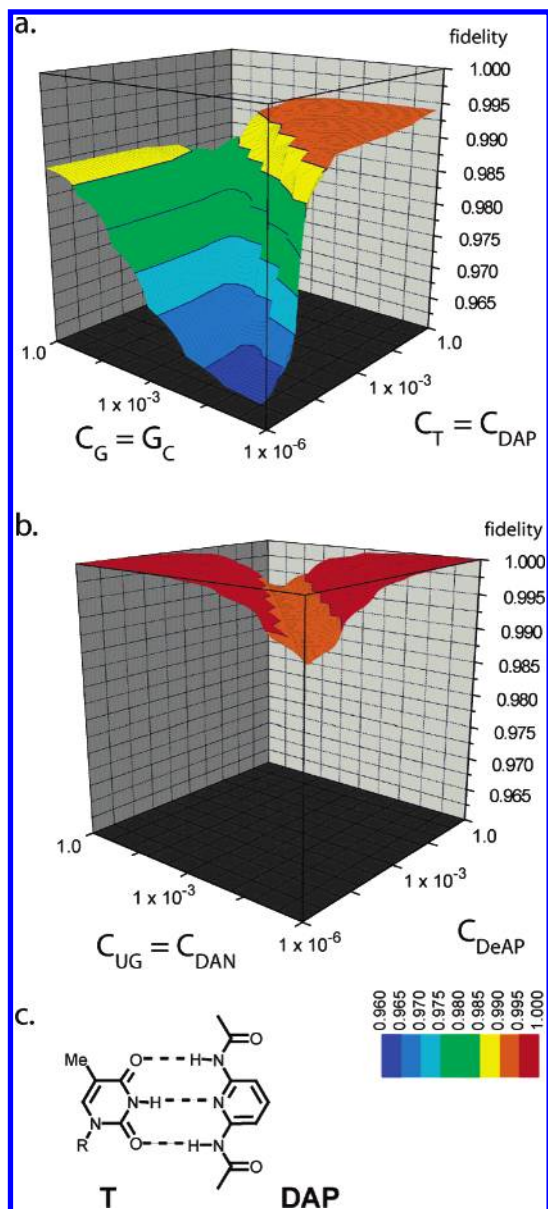
Figure 11. Fidelity plots for mixtures of (a) G·C and T·DAP and (b) UG·DAN and (DeAP)₂ complexes. C is analytical concentration (M). The former system and the methods used were published previously.[25] For part b, K_{assoc} = 1 × 10⁸ M⁻¹ was used for UG·DAN. Using K_{assoc} = 5 × 10⁷ M⁻¹ lowers the fidelity trough by only 0.003.

Conclusion

Multiply hydrogen-bonded complexes that can be readily prepared in large quantity have the potential to play an important role in a range of nanotechnological applications, including in supramolecular polymer chemistry. The DeAP and UPy dimers represent important members of the supramolecular toolkit that have already been applied in these areas. The DeAP·DAN and UPy·DAN heterocomplexes are among the first members to offer equally high stability but the ability to bring two different structures together. At some stoichiometries and concentrations, however, the fidelity is lower than ideal due to the ability of DeAP and UPy to strongly dimerize. In an effort to disfavor the DDAA form that strongly dimerizes, we explored different ring fusions and substituents on the ureidopyrimidinone nucleus. Recognizing that DNA bases, as carriers of the genetic code, tend toward tautomeric fixation the urea of guanosine (UG) was

examined both computationally and experimentally. It was found that indeed UG weakly dimerizes in chloroform solution (K_{dimer} < 300 M⁻¹) yet forms a highly stable complex with DAN (K_{assoc} ≈ 5 × 10⁷ M⁻¹) in the same solvent. The formation of the UG·DAN complex itself shows generally excellent fidelity unless highly nonstoichiometric ratios of the components are used. Mixtures of the UG·DAN heterocomplex and the DeAP dimer show outstanding fidelity across a broad concentration range at a wide range of stoichiometric ratios of the two associated species.

Reasonably convenient syntheses of the DAN unit are now available.[26] The synthesis of the UG unit described herein allows 10 g quantities to be prepared in four steps from commercially available guanosine with no chromatographic purification required. Structurally related units that perform similiarly but are even more accessible are currently in development. Additionally applications of the UG·DAN heterocomplex to a range of applications in supramolecular chemistry are under investigation and will be reported in due course.

Experimental Section

General experimental details can be found in the Supporting Information. The Supporting Information also contains detailed synthetic procedures and characterization data for compounds **11**−**17** and additional details for computational and complexation studies.

Heptanoic Acid (7-Heptanoylamino-[1,8]naphthyridin-2-yl)amide (3, R = C₆H₁₃). A mixture of 8.2 g (51 mmol) of 2,7-diaminonaphthyridine (**16**),[26] 38 mL (154 mmol) of heptanoic anhydride, and 626 mg (5.13 mmol) of DMAP in 250 mL of pyridine (250 mL) was heated at 100 °C for 2 days. The resulting mixture was cooled to room temperature. Pyridine was removed in vacuo, and excess heptanoic anhydride was removed by kugelrohr distillation. The crude material was dissolved in 200 mL of CHCl₃ and washed twice with 50 mL of H₂O, 20 mL of a saturated aqueous solution of sodium bicarbonate, and 50 mL of H₂O. The organic solution was dried over MgSO₄, filtered, and solvent removed in vacuo. The crude material was purified by column chromatography (SiO₂, R_f = 0.31, 95:5 CHCl₃:CH₃OH) to give 18.7 g (95%) of **3** as a white solid, mp 188−190 °C (CHCl₃); ¹H NMR (400 MHz, CDCl₃) δ 8.43 (2H, d, J = 8.8), 8.17 (2H, s), 8.12 (2H, d, J = 8.8), 2.45 (4H, t, J = 7.6), 1.78−1.71 (4H, m), 1.43−1.29 (12H, m) and 0.89 (6H, t, J = 6.8); ¹³C NMR (100 MHz, CDCl₃) δ 173.1, 154.5, 153.7, 139.3, 118.4, 113.4, 113.9, 38.0, 31.7, 29.0, 25.4, 22.7. MS m/z (electrospray ionization, ESI) 385.2601 [(M + H)⁺; C₂₂H₃₃N₄O₂ requires m/z 385.2604]. Anal. Calcd. for C₂₂H₃₂N₄O₂: C, 68.72; H, 8.39; N, 14.57. Found C, 68.58; H, 8.64; N, 14.05.

1-Butyl-3-[9-(6-hydroxymethyl-2,2-dimethyl-tetrahydro-furo[3,4-d][1,3]dioxol-4-yl)-6-oxo-6,9-dihydro-1H-purin-2-yl]-urea (UG, 4). To a milky solution of 12 g (31 mmol) of **7** and 6.55 g (37.7 mmol) of *p*-toluenesulfonic acid in 300 mL of acetone at room temperature was added 45.6 mL (314 mmol) of 2-dimethoxy propane. The resulting homogeneous mixture was stirred for 10 h at room temperature and concentrated ammonium hydroxide (NH₄OH) was added dropwise until no *p*-toluenesulfonic acid was visible by thin-layer chromatography. The precipitate was removed by filtration and the filtrate evaporated at reduced pressure. The residue was dissolved in 100 mL of CHCl₃ and washed with ca. 100 mL H₂O. The organic layer was removed, and the aqueous layer was washed with CHCl₃. The combined organic layers were washed with 200 mL of brine, dried over MgSO₄, and filtered. The solvent was removed on a rotary evaporator to afford 13.1 g (99%) of UG **4** as a fine, white powder, mp 177−179 °C (CHCl₃); ¹H NMR (400 MHz, DMSO-d₆) δ 11.94 (1H, s), 9.95 (1H, s), 8.04 (1H, s), 7.37 (1H, s), 5.97 (1H, d, J = 2.5), 5.18 (1H, dd, J = 2.3),

(26) Park, T.; Mayer, M. F.; Nakashima, S.; Zimmerman, S. C. *Synlett* **2005**, 1435−1436.

5.11 (1H, s), 4.94 (1H, dd, $J = 2.3$), 4.17 (1H, dd, $J = 2.3$), 3.51 (1H, br s), 3.14 (2H, quartet, $J = 6.5$), 1.50 (3H, s), 1.46−1.39 (2H, m), 1.30 (3H, s), 1.33−1.24 (2H, m), 0.87 (3H, t, $J = 7.4$); ^{13}C NMR (100 MHz, DMSO-d_6) δ 155.5, 149.2, 137.7, 120.0, 113.6, 90.2, 87.6, 84.7, 82.0, 62.1, 40.8, 32.0, 27.7, 25.9, 20.1, 14.3; MS m/z (ESI) 423.2006 [(M + H)$^+$, $C_{18}H_{27}N_6O_6$ requires m/z 423.1992].

2′,3′,5′-*O*-Acetyl Guanosine (5). By use of a modified procedure of that reported,[14] 20 mL (200 mmol) of acetic anhydride was added dropwise to a mixture of 19.1 g (67.5 mmol) of guanosine, 56.5 mL (405 mmol) of triethylamine, and 860 mg (7.0 mmol) of *N,N*-(dimethylamino)pyridine in 250 mL of CH_3CN at 0 °C. The mixture was stirred for 1 h and warmed to room temperature and stirred for 3 h. The reaction was quenched with 20 mL of methanol. The volume was reduced to 100 mL at reduced pressure, and diethyl ether was added dropwise for over 1 h to induce precipitation of a fine, white powder, which was collected by filtration and washed with diethyl ether. The powder was slurried in 250 mL of acetone and stirred at 50 °C for ca. 5 h. Filtration afforded 28.6 g (99%) of **5** as a fine white powder, mp 228−229 °C (CH_3CN); ^{1}H NMR (400 MHz, DMSO-d_6) δ 10.74 (1H, s), 7.92 (1H, s), 6.53 (2H, s), 5.96 (1H, d, $J = 6.5$), 5.76 (1H, t, $J = 5.5$), 5.47 (1H, t, $J = 5.5$), 4.35 (1H, dd, $J = 4.0, 10.0$), 4.29 (1H, dt, $J = 4.0, 10.0$), 4.23 (1H, dd, $J = 4.0, 10.8$). All other physical and spectroscopic data was identical to that previously reported.[14]

Acetic Acid 3,4-Diacetoxy-5-[2-(3-butylureido)-6-oxo-1,6-dihydro-purin-9-yl]-tetrahydro-furan-2-yl Methyl Ester (UG, 6). To a solution of 18.25 g (44.7 mmol) of **5** in 300 mL of DMF at 0 °C was added 1.7 g (42 mmol) of NaH (60% dispersion in mineral oil). The solution was slowly warmed to 70 °C and stirred for 2 h. The mixture was cooled to 0 °C, and 4.9 mL (44 mmol) of butylisocyanate was added. After 1 h, ca. 10 mL of a 5% (w/v) aqueous solution of hydrochloric acid was added to the mixture. The DMF was removed using a rotary evaporator equipped with high vacuum. The resulting solid was ground to a powder, washed with H_2O, and dissolved in 200 mL of $CHCl_3$. The solution was washed with water, and the aqueous layer was extracted with $CHCl_3$. The combined organic layers were washed with 200 mL of brine, dried over $MgSO_4$, and filtered. Removing the solvent in vacuo afforded 20.9 g (97%) of **6** as a white, fine powder, which was sufficiently pure to use in the next reaction. Further purification could be achieved by column chromatography (SiO$_2$, $R_f = 0.31$, 93:7 $CHCl_3$:CH_3OH), mp 103−105 °C ($CHCl_3$); ^{1}H NMR (400 MHz, CDCl$_3$) δ 12.65 (1H, s), 10.37 (1H, s), 7.93 (1H, s), 7.34 (1H, s), 6.07 (1H, t, $J = 9.4$), 6.01 (1H, t, $J = 5.1$), 5.60 (1H, br t, $J = 9.4$), 4.37 (1H, dd, $J = 7.6$), 4.37 (1H, s), 4.23 (1H, dd, $J = 7.6$), 3.30 (2H, quartet, $J = 6.4$), 2.10 (3H, s), 2.07 (3H, s), 1.99 (3H, s), 1.60−1.52 (2H, m), 1.41−1.32 (2H, m), 0.93 (3H, t, $J = 7.6$); ^{13}C NMR (100 MHz, CDCl$_3$) δ 177.8, 169.9, 169.9, 157.019, 155.6, 150.4, 149.5, 138.3, 120.7, 87.0, 80.3, 72.3, 70.9, 63.1, 40.0, 31.9, 20.8, 20.7, 20.7, 20.1, 13.9; MS m/z (ESI) 509.2013 [(M + H)$^+$, $C_{21}H_{29}N_6O_9$ requires m/z 509.1996]. Anal. Calcd. for $C_{21}H_{28}N_6O_9$: C, 49.60; H, 5.55; N, 16.53. Found C, 49.50; H, 5.60; N, 16.05.

1-Butyl-3-[9-(3,4-dihydroxy-5-hydroxymethyl-tetrahydro-furan-2-yl)-6-oxo-6,9-dihydro-1H-purin-2-yl]-urea (UG, 7). To a solution of 11.3 g (22.3 mmol) of **6** in 100 mL of CH_3OH at room temperature was added 5.42 g (100 mmol) of sodium methoxide producing a white precipitate. The mixture was stirred for 10 h at room temperature and ca. 10 mL of a 5% (w/v) aqueous solution of HCl was added to the

mixture. To the homogeneous mixture was added dropwise 200 mL of H_2O precipitating crude product which was collected by filtration, washed with ethanol, ethyl acetate, diethyl ether, and pentane to afford 8.4 g (99%) of **7** as a fine, white powder, mp 242−243 °C (CH_3OH); ^{1}H NMR (400 MHz, DMSO-d_6) δ 11.91 (1H, s), 9.95 (1H, s), 8.14 (1H, s), 6.93 (1H, t, $J = 5.6$), 5.71 (1H, d, $J = 5.6$), 5.45 (1H, d, $J = 5.9$), 5.15 (1H, d, $J = 4.9$), 5.01 (1H, t, $J = 5.0$), 4.39 (1H, dd, $J = 5.0$), 4.09 (1H, dd, $J = 4.3$), 3.88 (1H, dd, $J = 3.5$), 3.66−3.58 (1H, m), 3.56−3.49 (1H, m), 3.13 (2H, qu, $J = 6.6$), 1.46−1.39 (2H, m), 1.33−1.24 (2H, m), 0.87 (3H, t, $J = 7.4$); ^{13}C NMR (100 MHz, DMSO-d_6) δ 155.8, 155.6, 149.8, 149.4, 137.8, 119.2, 87.6, 85.9, 74.6, 70.8, 61.8, 39.4, 31.9, 20.0, 14.3. MS m/z (ESI) 383.1691 [(M + H)$^+$ $C_{15}H_{23}N_6O_6$ requires m/z 383.1679].

UG−Dye343 Conjugate (18). A mixture of 57 mg (0.2 mmol) of coumarin 343, 51 mg (0.26 mmol) of EDCI, and 12 mg (0.04 mmol) of DPTS (DMAP-*p*-toulenesulfonic acid complex) in 10 mL of DMF was stirred at room temperature for 1 h. A solution of 84.4 mg (0.2 mmol) of **7** in 5 mL of DMF was added, and the mixture was stirred at room temperature for 15 h. The solvent was removed by a rotary evaporator equipped with high vacuum and the residue dissolved in 20 mL of chloroform. The solution was washed with 20 mL of H_2O, and the aqueous layer was extracted three times with 20 mL of $CHCl_3$. The combined organic layers were washed with 20 mL of brine, dried over $MgSO_4$, filtered, and the solvent removed with rotary evaporator. The crude material was purified by column chromatography (SiO$_2$, $R_f = 0.30$, 95:5 $CHCl_3$:CH_3OH) to give 68 mg (50%) of **18** as an orange solid: ^{1}H NMR (500 MHz, CDCl$_3$) δ 12.23 (1H, s), 10.25 (1H, s), 8.24 (1H, s), 7.97 (1H, s), 7.27 (1H, s), 6.89 (1H, s), 6.06 (1H, s), 5.33 (1H, d, $J = 5.9$), 5.23 (1H, dd, $J = 2.4$), 4.88 (1H, dd, $J = 2.4$), 4.94 (1H, dd, $J = 5.9$), 4.62 (1H, dd, $J = 2.4$), 3.33−3.27 (6H, m), 2.77−2.69 (4H, m), 1.93 (4H, m), 1.58 (3H, s), 1.55 (2H, t, $J = 7.5$), 1.38 (2H, t, $J = 7.5$), 1.33 (3H, s), 0.92 (3H, t, $J = 7.4$); ^{13}C NMR (125 MHz, CDCl$_3$) δ 164.9, 159.4, 155.2, 153.8, 150.2, 149.8, 149.6, 148.65, 138.1, 127.7, 120.3, 120.2, 114.3, 107.9, 105.7, 104.8, 91.2, 85.8, 85.3, 81.8, 64.0, 50.6, 50.1, 40.0, 32.0, 27.5, 27.3, 25.5, 21.1, 20.3, 20.2, 14.0. MS m/z (ESI) 690.2894 [(M + H)$^+$ $C_{34}H_{40}N_7O_9$ requires m/z 690.2888].

Supporting Information Available: General experimental details, detailed synthetic procedures and characterization data for compounds **11**-**17**, details on the X-ray analysis of **6** including a cif file, and additional experimental details on computational and complexation studies. This material is available free of charge via the Internet at http://pubs.acs.org.

JA0545517